THE EFFECT OF SMALL DEVIATORIC STRESSES
ON CAVERN CREEP BEHAVIOR

Brouard Benoit

Brouard Consulting – 101 rue du Temple, 75003 Paris, France

Bérest Pierre

LMS, Ecole Polytechnique Paris Tech – Route de Saclay, 91128 Palaiseau, France

Karimi-Jafari Mehdi

Geostock – 7 rue E. et A. Peugeot, 92563 Rueil-Malmaison, France

SUMMARY

One-year-long creep tests performed under very small deviatoric stresses and a 6-month-long brine outflow test performed in a shallow salt cavern are described. Both strongly suggest that the rate of salt creep under small deviatoric stresses ($\sigma < 5$ MPa) is likely to be much faster than what usually is inferred from laboratory tests performed under higher mechanical loadings. Numerical computations prove that cavern-closure prediction has potential significant consequences.

1. THE STANDARD NORTON-HOFF LAW

1.1. The Micro-Mechanisms Governing Salt Creep

Hunsche (1984), Munson and Dawson (1984), Langer (1984) and Blum and Fleischman (1988) have discussed the micro-mechanisms that govern salt creep. Langer (1984) states that:

> *Reliable extrapolation of the creep equations over long period of time and at low deformation rates can only be carried out on the basis of deformation mechanisms. The construction of a deformation-mechanism map is an essential preliminary.*

Such a map (adapted from Munson and Dawson, 1984) is presented in Figure 1. The governing creep mechanism is indicated for each domain of the Temperature-Deviatoric Stress plane; the homologous temperature is the temperature (in Kelvin) divided by salt melting temperature (1077 K); and μ is the shear modulus. Two rectangles also are drawn; the $[0-120癈] \times [5-20\text{MPa}]$ rectangle is the domain in which laboratory tests generally are performed. As will be seen, the $[0-120癈] \times [0-5\text{MPa}]$ rectangle is the domain of temperature and deviatoric stress *actually* experienced in the vicinity of a salt cavern during most of its lifetime. (Gas storage caverns, which experience large pressure changes, are an outstanding exception.) Except for the upper part of the first rectangle, in which dislocation creep is the dominant mechanism, the micro-mechanism that governs creep in these two rectangles is poorly known. However, Spiers et al. (1990) suggested that, in the low stress range, pressure solution is an important mechanism (see Section 1.3).

In other words, prediction of the mechanical behavior of a cavern is based on empirical data. Furthermore, as tests are performed in the 5-20 MPa deviatoric stress range, empirical creep laws inferred from laboratory testing must be extrapolated to the 0-5 MPa deviatoric stress range (the range of primary interest when considering cavern behavior), for which few or no actual data are available.
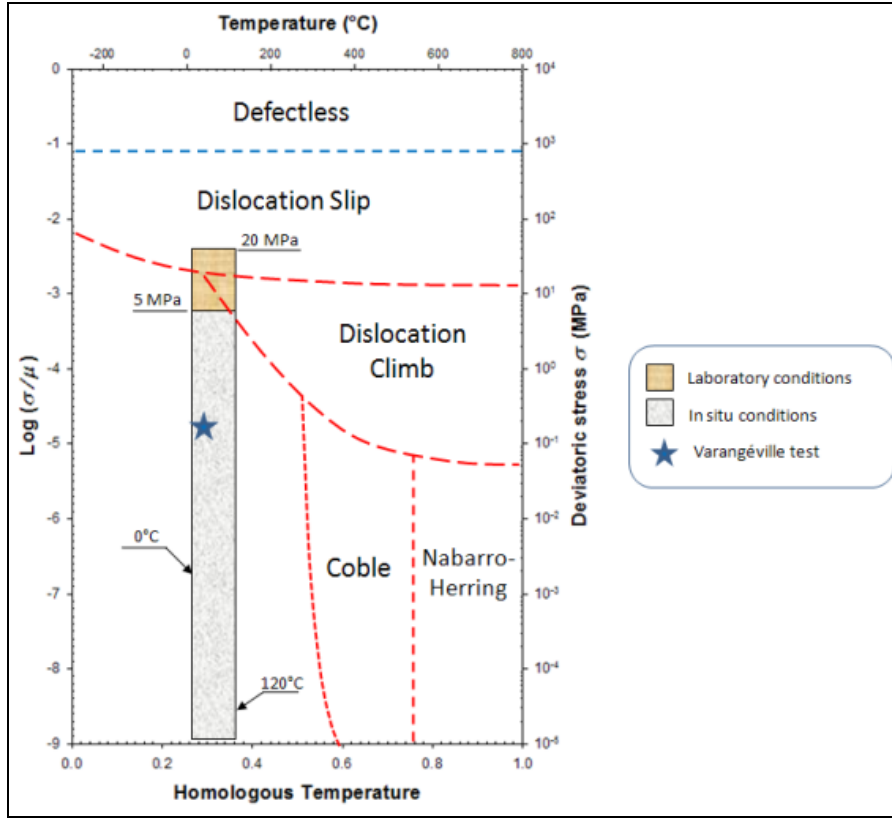
Figure 1. Mechanism Map (after Munson and Dawson, 1984): Stress and temperature conditions during the test described in Section 2.2 are represented by a star.

1.2. Norton-Hoff Law and Small Deviatoric Stresses

Steady-state creep rates, as observed during laboratory tests performed in the 5-20 MPa range, often are fitted against the applied deviatoric stress. In the range of temperatures experienced in most salt caverns, the Norton-Hoff law captures the main features of the steady-state behavior of salt:

$$\dot{\varepsilon}^{ss} = A\exp\left(-\frac{Q}{RT}\right)\sigma^{n} \qquad (1)$$

where n belongs to the range $n = 3\text{-}6$. When the deviatoric stress is $\sigma = 10\,\text{MPa}$, a typical steady-state strain rate is $\dot{\varepsilon}^{ss}_{10\,\text{MPa}} = 10^{-10}\,\text{s}^{-1}\ \left(3\times10^{-3}\,\text{yr}^{-1}\right)$; in fact, most observed rates range from $\dot{\varepsilon}^{ss}_{10\,\text{MPa}} = 10^{-11}\,\text{s}^{-1}$ to $\dot{\varepsilon}^{ss}_{10\,\text{MPa}} = 10^{-9}\,\text{s}^{-1}$. When $n = 3$ is allowed, the (extrapolated) steady-state strain rate is $\dot{\varepsilon}^{ss}_{10\,\text{MPa}} = 10^{-13}\,\text{s}^{-1}$ when the deviatoric stress is $\sigma = 1\,\text{MPa}$; it is $\dot{\varepsilon}^{ss}_{10\,\text{MPa}} = 10^{-16}\,\text{s}^{-1}$ when the deviatoric stress is $\sigma = 0.1\,\text{MPa}$. This last strain rate is exceedingly slow: after a period lasting 300,000 years, the cumulated strain is $\varepsilon = 10^{-3}$. Such slow strain rates cannot be observed in the laboratory.

1.3. Norton-Hoff Law and Cavern Convergence Computations

Equation (1) holds for creep tests performed on cylindrical samples. It needs to be generalized to 3D situations:

$$\&_{ij} = \frac{1+\nu}{E}\&_{ij} - \frac{\nu}{E}\&_{kk}\delta_{ij} + \frac{3}{2}A^*\left(\sqrt{3J_2}\right)^{n-1}s_{ij} \tag{2}$$

where $A^* = A\exp(-Q/RT)$; s_{ij} is the deviatoric stress tensor, and $J_2 = s_{ij}s_{ji}/2$ is the second invariant of the deviatoric stress tensor. Consider the case of an idealized spherical cavern of radius a in an infinite elasto-visco-plastic medium. The geostatic pressure at cavern depth is P_∞. At time $t = 0$, the cavern is submitted to an internal pressure, $P_c < P_\infty$, which, later ($t > 0$), is kept constant. In a brine-filled cavern 1000-m deep, $P_\infty - P_c = 10$ MPa is typical. After the initial rapid pressure change, the cavern experiences a transient phase during which the deviatoric stresses decrease, and, after a (long) period of time, a steady state is reached. The steady-state volume-loss rate and the steady-state deviatoric stress distribution can be computed easily (see Bérest et al., 2008):

$$\frac{\&V^{NH}}{V}\bigg|_{SS} = -\frac{3}{2}A^*\left[\frac{3}{2n}(P_\infty - P_c)\right]^n \tag{3}$$

$$\sqrt{3J_2}\bigg|_{SS}^{NH} = \frac{3}{2n}(P_\infty - P_c)\left(\frac{a}{r}\right)^{3/n} \tag{4}$$

Formula (4) links the deviatoric stress ($\sqrt{3J_2}$) to the pressure difference ($P_\infty - P_c$) and to the distance (r) to cavern centre. It is interesting to compare this "steady-state" stress distribution to the "elastic" stress distribution that is observed immediately after the beginning of the transient phase, when the internal pressure $P_c < P_\infty$ is applied:

$$\sqrt{3J_2}\bigg|_{SS}^{EL} = \frac{3}{2}(P_\infty - P_c)\left(\frac{a}{r}\right)^3 \tag{5}$$

Two conclusions can be drawn from these equations.

First, the perturbation to the natural isotropic state of stress penetrates much deeper inside the rock mass for the steady-state solution, as $n > 1$. *Significant deviatoric stresses are present in a much larger rock volume when the steady-state stress distribution is compared to the elastic distribution.*

Second, the deviatoric stress at the cavern wall ($r = a$) is divided by n when the steady-state stress distribution is compared to the elastic distribution. *Deviatoric stresses in the salt mass are small when the steady-state distribution is reached.* For instance, in a 600-m-deep cavern, $P_\infty - P_c = 6$ MPa; when $n = 3$, the maximum deviatoric stress in the rock mass is $\sqrt{3J_2}\big|_{SS}^{NH}(r = a) = 3$ MPa. (It is $\sqrt{3J_2}\big|_{SS}^{NH}(r = a) = 1.8$ MPa when $n = 5$.)

It can be inferred from these conclusions that studying the effects of small deviatoric stresses (and slow strain rates) is especially important when assessing cavern steady-state creep closure.

2. THE SIGNIFICANCE OF SMALL DEVIATORIC STRESSES

2.1. Pressure-Solution Creep

When fitted against the results of laboratory tests performed in the domain $[0-120℃]\times[5-20\text{MPa}]$, the Norton-Hoff law is purely empirical in origin. Extrapolation of the Norton-Hoff law to a range of stresses smaller than the range of stresses against which this law was fitted cannot be substantiated by micro-mechanism analysis.

However, Spiers et al. (1990) observed that pressure-solution creep, an important deformation mechanism in most rocks in the Earth's crust, is especially rapid in rock salt. Theoretical findings strongly suggest that, for this mechanism, the relation between deviatoric stress and strain rate is linear. The strain rate observed during laboratory tests is the sum of the strain rates generated by two mechanisms: dislocation creep, and pressure-solution creep. At low temperature ($T < 100℃$), dislocation creep is the dominant mechanism in the domain $\sigma > 10$ MPa; when smaller deviatoric stresses are considered, pressure-solution creep usually is dominant. In fact, as emphasized by Uraï and Spiers (2007, p.151):

> "... the relative importance of each process depends strongly on variables such as temperature, confining pressure, grain size, solid solution impurities and second phase content and, importantly, on the presence of sufficient water in grain boundaries to enable solution-precipitation phenomena".

According to Uraï and Spiers (2007), the Norton-Hoff (N-H) law typically should be modified in such a way that

$$\dot{\varepsilon} = A\exp\left(-\frac{Q}{RT}\right)\sigma^n + \frac{b}{TD^3}\exp\left(-\frac{\overline{Q}}{RT}\right)\sigma \tag{6}$$

where b and $\overline{Q}/R$ are constants, and D is the grain diameter. One practical consequence of this is that the creep rate experienced by a salt sample submitted to small deviatoric stresses should be much faster than that extrapolated from the Norton-Hoff law ($b = 0$) fitted on standard laboratory tests (i.e., performed in the range $\sigma = 5$-20 MPa).

2.2. Laboratory Evidence

The effect of small deviatoric stresses (hence, slow creep rates — say, $\dot{\varepsilon} < 10^{-10}\text{s}^{-1}$) has not been investigated widely in the literature, despite their role with regard to geological deformations. Hunsche (1988) performed tests lasting 10 days during which an axial load of 0.57 MPa was applied on a cylindrical sample; the observed strain rate typically was $7\times10^{-12}\text{s}^{-1}$. In fact, accurate long-term creep tests are possible only when there is accurate measurement of the sample's height change (10^{-3}–10^{-2} micrometer), when the applied load remains constant and, importantly, when the temperature and hygrometry experience very small changes for the duration of the test. Bérest et al. (2005) describe such experiments, performed in deep underground galleries (to take advantage of stable temperature and hygrometry) and using extremely accurate sensors and dead-weight loading. They found (Figure 2) that a typical steady-state strain rate when the applied stress was $\sigma = 0.108$ MPa was

$$\dot{\varepsilon} = 1.4\times10^{-12} \text{ s}^{-1} \tag{7}$$

This rate is exceedingly slow, but it is much faster — by 3 or 4 orders of magnitude — than the creep rate that is extrapolated from tests performed on the same natural rock salt when a deviatoric stress, $\sigma = 5 - 20$ MPa, is applied on a sample.
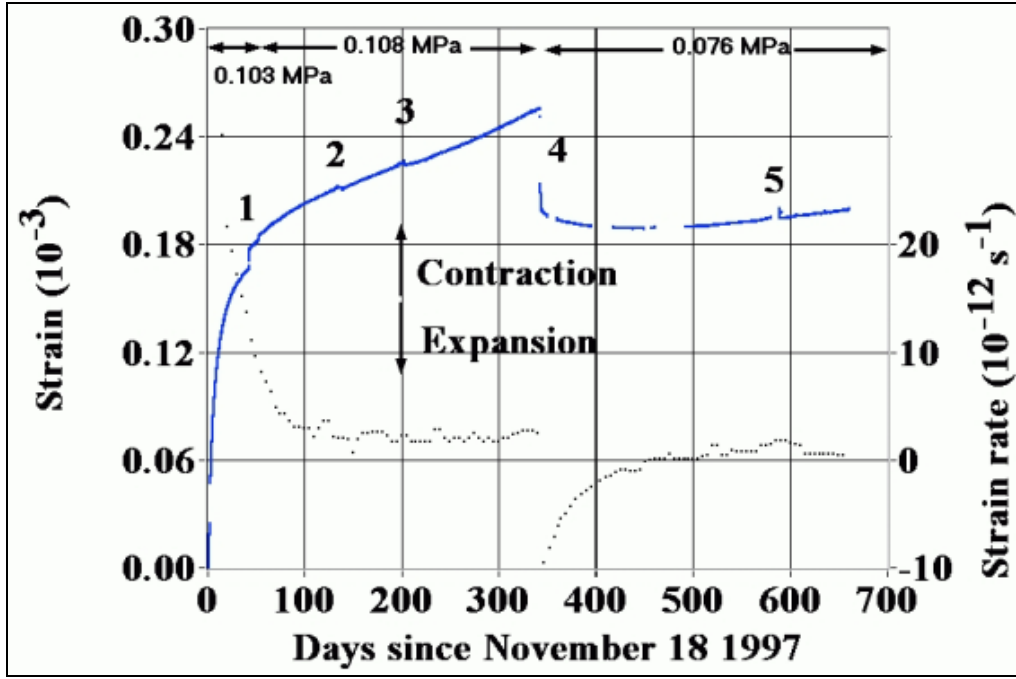
Figure 2. A 22-month-long creep test performed on a salt sample. When the applied stress was 0.108 MPa, the axial creep rate was $1.4 \times 10^{-12}\,\mathrm{s}^{-1}$ — a surprisingly fast rate.

2.3. Practical Consequences for a Cavern

The Norton-Hoff law can be represented in the ($\log \dot{\varepsilon}^{ss} - \log \sigma$) plane by a straight line with a slope of n. This curve correctly fits data in the domain $\sigma = 5 - 20$ MPa, but it widely underestimates the actual creep rate in the domain $\sigma < 5$ MPa. It is suggested that the mechanical behavior be described by the following bi-linear law:

$$\sigma > S: \qquad \dot{\varepsilon}^{ss} = A^*\sigma^n \tag{8}$$

$$\sigma < S: \qquad \dot{\varepsilon}^{ss} = B^*\sigma \tag{9}$$

In other words, when the deviatoric stress is large enough, the standard Norton-Hoff law ($n \neq 1$) holds; when the deviatoric stress is small, the Newtonian law ($n = 1$) for viscous fluids holds. For continuity, $\dot{\varepsilon}^{ss}(\sigma = S) = A^*S^n = B^*S$.

This bi-linear law clearly is simplistic. It would be more realistic to assume that the transition from Dislocation Creep to Pressure Solution is gradual. However, this bi-linear model allows for simple computations. The objective of this paper is to highlight the significance of small deviatoric stresses; precise prediction will be possible when the database is larger.

Consider an idealized spherical cavern and steady-state creep closure: when the cavern is deep enough, the rock mass is divided in two zones. In the zone closest to the cavern, deviatoric stresses are large, and (8) holds. Farther from the cavern, deviatoric stresses are small, and (9) holds. The steady-state cavern closure rate can be computed easily (Bérest et al., 2008):

$$\left.\frac{\dot{V}}{V}\right|_{SS}^{BL} = -\frac{3}{2}A\left\{\frac{3}{2n}\left[P_\infty - P_c + \frac{2}{3}(n-1)S\right]\right\}^n = \left[1 + \frac{2(n-1)S}{3(P_\infty - P_c)}\right]^n \times \left.\frac{\dot{V}}{V}\right|_{SS}^{NH} \tag{10}$$

For instance, $n = 3$, $S = 1.5$ MPa, $P_\infty - P_c = 10$ MPa and

5

$$\left.\frac{\overset{\&}{V}}{V}\right|_{SS}^{BL} = 1.7 \left.\frac{\overset{\&}{V}}{V}\right|_{SS}^{NH}$$

When plausible values of n and S are selected, the creep closure rate is significantly faster when the Norton-Hoff creep law is modified slightly to take into account the effect of small deviatoric stresses.

3. FIELD EVIDENCE

3.1. A Comment on Field Evidence

Numerical computations currently are performed to assess the creep closure rates of salt caverns and cavern stability. These computations use constitutive laws that are based on empirical data provided by laboratory tests. In fact, as explained above, the deviatoric stresses experienced in a salt mass in the neighborhood of a salt cavern are significantly smaller than the deviatoric stresses generally applied to salt samples in the laboratory. The constitutive laws fitted against the results of laboratory tests may be irrelevant when predicting the behavior of a salt cavern.

In this context, field evidence should be helpful. Unfortunately, it is difficult to compare any computational result to the actual behavior of a salt cavern other than in a qualitative manner. Bérest et al. (2006) observed that, in most cases, it is difficult to measure cavern shape or volume changes directly. In fact, during most in-situ mechanical tests, what is measured is the evolution of the wellhead pressure or the flow rate of the expelled [liquid] volume. The evolution of these quantities is influenced not only by purely mechanical effects: factors such as cavern brine warming (or cooling), additional dissolution, brine micro-permeation through the cavern walls and fluid leaks through the casing also play roles. In many cases, for instance, the effects of cavern brine warming are more significant than the effects of cavern-creep closure. For this reason, interpreting an in-situ "mechanical" test is often difficult.

In other words, monitoring cavern behavior does not provide strong evidence for (or against) any type of governing mechanism in the low stress range. However, some interesting attempts have been made by Breunesse et al. (2003), who interpreted subsidence data above salt caverns. In the case of a salt dry mine, Campos de Orellana (1998) systematically examined pillar creep rates and convincingly proved that field data were better explained when faster rates were associated with small applied stresses. A comprehensive discussion of available evidence, both from laboratory experiments and field observations, can be found in Uraï and Spiers (2007).

In the following, a brine-outflow test performed in a 250-m deep cavern is described. At such depth, it can be expected that geostatic pressure and deviatoric stresses in the vicinity of a cavern will be relatively small.

3.2. An Overview of the SG13-SG14 Caverns

The Compagnie des Salins du Midi et salines de l'Est (CSME) has operated a brine field, described by Buffet (1998), at Gellenoncourt in Eastern France since the beginning of the 20th Century. . It is located at the eastern (shallowest) edge of the Keuper bedded-salt formation of Lorraine-Champagne, in which the salt thickness is 150 m.

During the first half of the 20th Century, single wells were brined out. After 1965, the hydrofracturing technique was used. For this brine field, cased and cemented wells are drilled to a depth of 280-300 m. The horizontal distance between two neighboring wells typically is 100 to 150 m. A link is created between the two caverns at well bottom through hydrofracturing. Water then is injected in one well, and brine is withdrawn from the other. Caverns grow, and their roofs reach the upper part of the salt formation, whose top is approximately 220-m deep.

Brining stops when the cavern roof is 10 m below the salt roof. This 10-m-thick salt slab is left to protect the overlying strata, which are prone to weathering when in contact with brine (Buffet, 1998).

The SG13 and SG14 wells were drilled in May 1975, and operated as brine-production caverns from July 1976 to June 1977 (SG13), and from October 1978 to July 1980 (SG14). After some time, the two caverns coalesced, and SG13-SG14 now is composed of two parts connected by a large link; hydraulically, they can be considered as a single cavern. From the latest sonar measurements (2000), it was inferred that the volumes of SG13 and SG14 are 107,000 m^3 and 34,000 m^3, respectively. (In fact, the overall volume is larger, as be seen below). A 3D view of the caverns is provided in Figure 3.
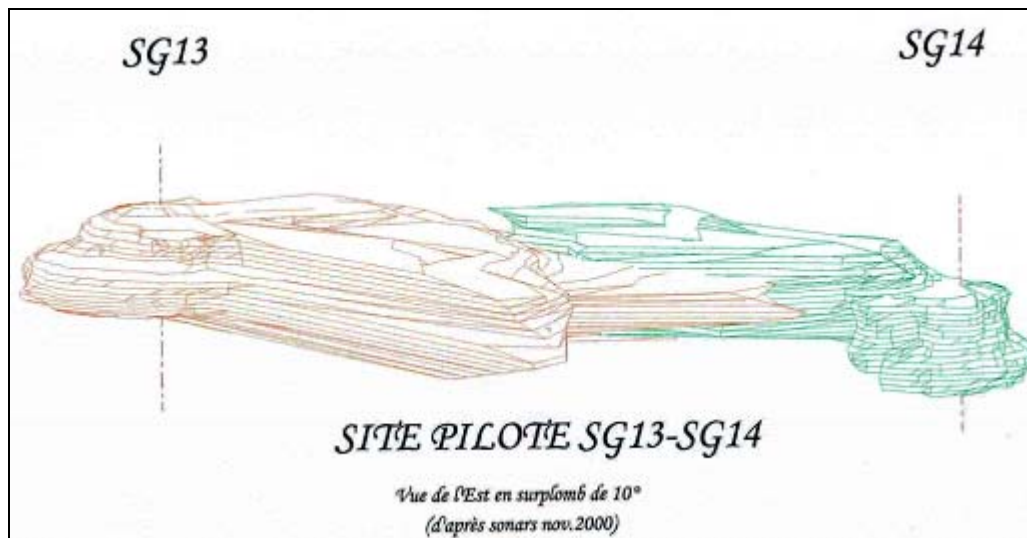

Figure 3. 3D sonar view of caverns SG13-SG14.

3.3. Cavern Compressibility Test

On July 3, 2009, cavern compressibility was measured by depressurizing SG13 from 0.18 MPa to zero. Brine was vented from the cavern to a 500-liter container. An accurate flow-meter had been set at the SG13 wellhead, and cavern pressure was measured at the SG14 wellhead. Figure 4 shows the expelled-brine-volume versus SG14-pressure-drop curve. The slope of this curve is the (as-measured) cavern compressibility, or $\beta V = 129.55$ m^3/MPa. When compared to cavern "sonar" volumes, this figure is relatively high, as the cavern compressibility factor generally is in the range $\beta = 4 - 5 \times 10^{-4}$/MPa (Bérest et al., 1999). As the sonar could "see" only the walls of the caverns that are reached by the sonar beams, the actual cavern volume probably was underestimated by sonar measurements. This last assumption is supported by the value of the cumulated volume of injected water during cavern operation, which strongly suggests that the actual cavern volume might be as large as $V = 240,000$ m^3, a figure consistent with the as-measured cavern compressibility.
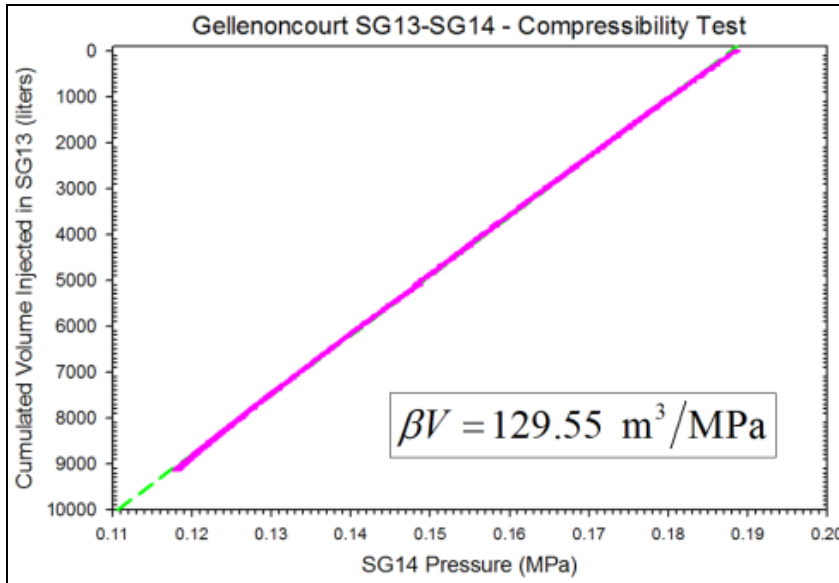
Figure 4. Cavern compressibility measurements.

3.4. A Brine Outflow Test

The cavern creep-closure rate can be assessed through "brine-outflow" tests. Brine-outflow tests consist of opening the cavern and measuring the flow of liquid (brine or hydrocarbon) expelled from the wellhead (Figure 5).
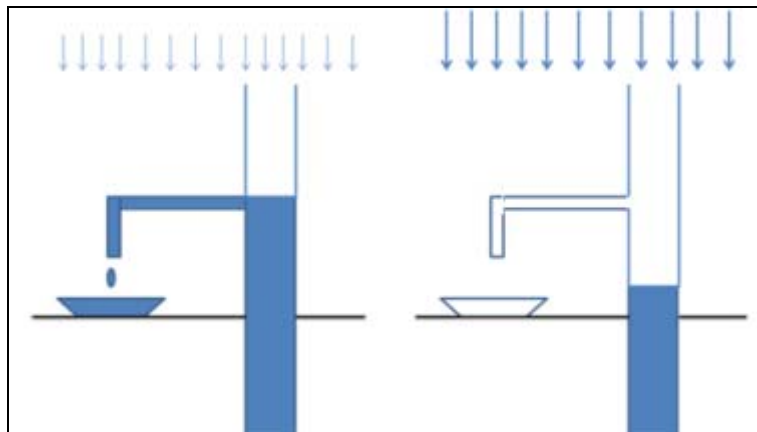

Figure 5. Brine-outflow test: left, the atmospheric pressure is low, and brine flows from the cavern; right, atmospheric pressure rapidly increases, and no brine flow is observed.

Outflow tests have been described in the literature; see, for example, Clerc-Renaud and Dubois (1980), Hugout (1988), Brouard et al. (2004) and Gaulke et al. (2007).

The liquid-outflow rate is governed by two main phenomena:

    (1) cavern-creep closure rate; and

    (2) cavern-brine thermal expansion.

Two other phenomena also may play a role:

    (3) brine micro-permeation through the cavern walls; and

    (4) brine leaks through the casing and casing shoe.

8

However, the significance of leaks and micro-permeation during an outflow test often is minor. During a brine-outflow test, the central tubing is open at ground level and is filled with saturated brine; consequently, the cavity pressure is halmostatic. It is well known from Mechanical Integrity Tests (Bérest et al., 2007) that leaks and micro-permeation are large only when the cavern pressure is much higher than halmostatic.

Several more-or-less periodic phenomena also influence the brine-outflow rate:

      (5) atmospheric pressure variations;

      (6) ground-level temperature variations; and

      (7) Earth tides.

In a deep cavern, the cavern closure rate and the brine thermal-expansion rate are fast, and the other phenomena are not able to make the brine outflow vanish. In a shallow cavern, the closure rate and the thermal expansion rate often are slow, and the other phenomena play a large role: brine outflow vanishes periodically — e.g., when the atmospheric pressure drastically increases (Figure 5).

However, when the testing period is sufficiently long (say, at least several weeks), the average effect of these periodic phenomena is nil, and the average brine-outflow rate mainly depends on the cavern-creep closure rate and the cavern-brine thermal expansion.

3.5. Outflow Measurement System

A general view of the outflow measurement system is given in Figure 6. A cabin was installed above the wellhead for security reasons. A solar panel was set on the cabin roof (upper-right part of Figure 6) to provide an energy supply. (The cavern wellheads are located far from the brine field station.) A more detailed view of the brine measurement system is provided in the lower-left part of Figure 6, and the upper part of the 7" casing is shown on the lower right part of Figure 6. A hole (Figure 7) was drilled through the steel tube to allow evacuation of the brine to a plastic container whose weight is measured every minute. When this container is filled with brine, an electric valve automatically triggers container venting. A plastic tube was set above the 7" casing to prevent overflow. (During a rapid drop in atmospheric pressure, brine flow sometimes may increase very rapidly, generating a brine overflow when the small hole is not able to accommodate the rapid flow increase. The air/brine interface slightly rises above the hole in the plastic tube; after a couple of minutes, the excess brine is evacuated to the container through the hole and the interface lowers to hole level.)

3.6. Average Brine-Flow-Rate

The test started on July 23, 2008. The cumulated volume of expelled brine as a function of time is shown in Figure 8. Some uncertainty does exist; for instance, the brine outflow during container venting periods is not taken into account. The average brine-outflow rate (i.e., the overall amount of brine expelled during the testing period divided by the testing period duration) is $Q_{av} \approx 12$ liters/day .

When this flow is compared to the cavern "sonar" volume, or $V = 240,000$ m^3, the relative convergence rate is $\dot{V}/V = 5.8 \times 10^{-13}$ s$^{-1} = 1.8 \times 10^{-5}$ yr^{-1}. In the following sections, it is proven that this flow rate can be considered representative of the cavern-creep closure rate, as, on one hand, thermal expansion is likely to be negligible and, on the other hand, fluctuations in brine flow can be explained by atmospheric pressure variations, ground-level temperature variations and Earth tides — three phenomena whose effects, when averaged over a period lasting several months — also are negligible.

Figure 6. Brine flow-rate measurement system, from left to right and top to bottom: general overview; solar panel; plastic container; 7'' upper part.
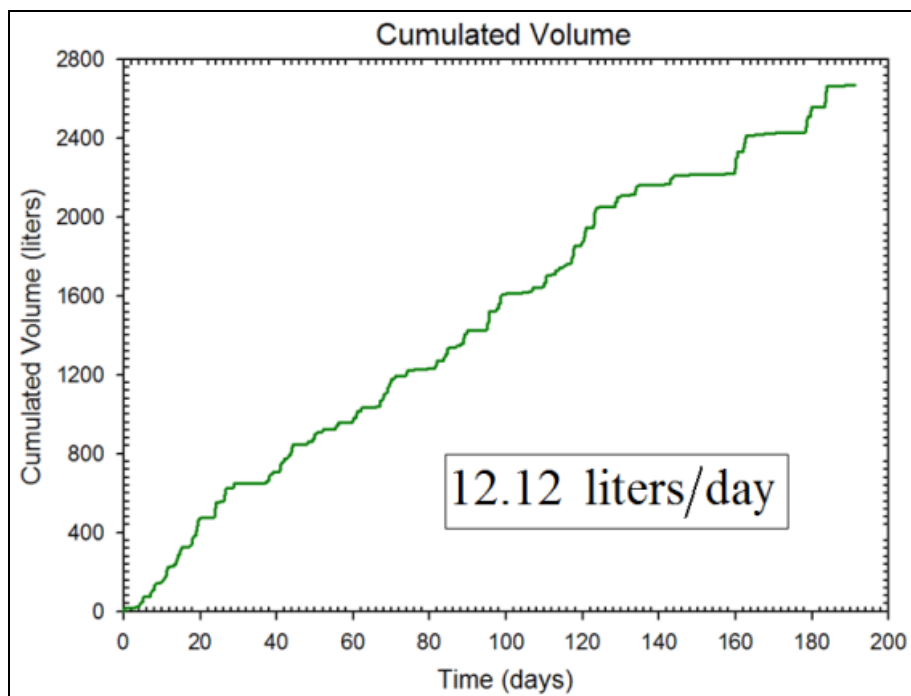
Figure 7. Venting hole in the 7" tube.

Figure 8. Cumulated outflow volume during a 200-day period.

3.7. Brine Thermal Expansion

Brine thermal expansion is a real concern, as its effects often are large during a brine-outflow test (and a shut-in pressure test as well; see Bérest et al., 2006). Brine thermal expansion (or contraction) results from the gap between the temperature of the cavern brine and the geothermal temperature of the rock. When the cavern brine is colder than the rock mass, heat is transferred from the rock mass to the cavern, resulting in brine warming (Bérest et al., 2001). Conversely, when the brine is warmer than the rock mass, heat is transferred from the brine to the rock mass, resulting in brine cooling. Brine warming (or cooling) generates brine expansion

11

(or contraction), which contributes to brine outflow. This process is slow — and even slower in a larger cavern. In a 240,000-m^3 cavern, it is expected that, after approximately 10 years, the initial temperature gap is divided by a factor of 4. For the SG13-SG14 cavern, soft water injected during the leaching process was slightly warmer (20 °C) than the rock geothermal temperature, which typically is 16.6 °C at cavern depth. The initial gap was small. Moreover, the cavern had been kept idle for nearly 30 years by the time after the brine-outflow test began. It was believed that thermal equilibrium nearly was reached at that time.
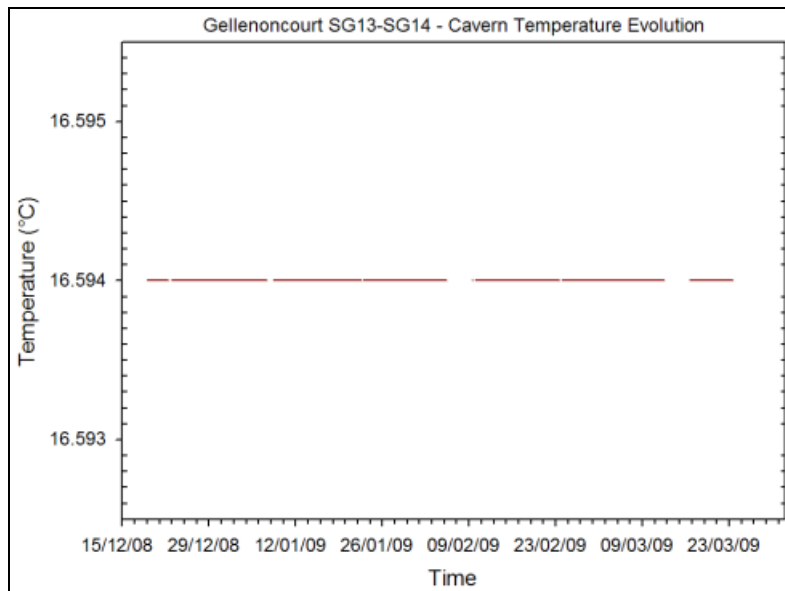

Figure 9. Cavern temperature evolution from December 2008 to March 2009.

However, by December 2008, a temperature gauge was lowered into the SG13 well to check temperature evolution (represented in Figure 9). The temperature apparently is perfectly constant during the period December 2008 – March 2009; however, this period is too short to allow for definite conclusions. (Although the temperature gauge resolution is 1/1000 °C, the accuracy of the temperature gauge is $\Delta\theta = 1/100$ °C; for the 4-month temperature measurement period, it can be inferred that temperature rate certainly is slower than $\dot{\theta} = 0.03°$ C/yr and that the brine expansion/contraction rate certainly is slower than $\alpha V \dot{\theta} = 10$ litres/day — possibly much slower.) It is believed that a longer test period will prove that the actual temperature rate is exceedingly slow.

3.8. Brine Flow-Rate Fluctuations

The *average* brine flow-rate, which is representative of the cavern creep-closure rate, was computed in Section 3.6 to be 12 liters/day. However, from Figure 8, it can be seen that the brine flow-rate is far from being constant. In fact, large fluctuations can be observed: periodically, the brine flow-rate increases to several hundreds of liters per day — i.e., larger than the average flow rate by one or two orders of magnitude (see Figure 10). Conversely, for most of the time, the flow-rate is nil: no flow is expelled from the cavern, and the air/brine interface drops down into the well. In fact, the brine-outflow rate is influenced by cavern creep closure and brine thermal expansion, which were discussed earlier, as well as by brine permeation, brine leaks, atmospheric pressure variations, ground-level temperature variations and Earth tides, which are discussed briefly in the following sections.
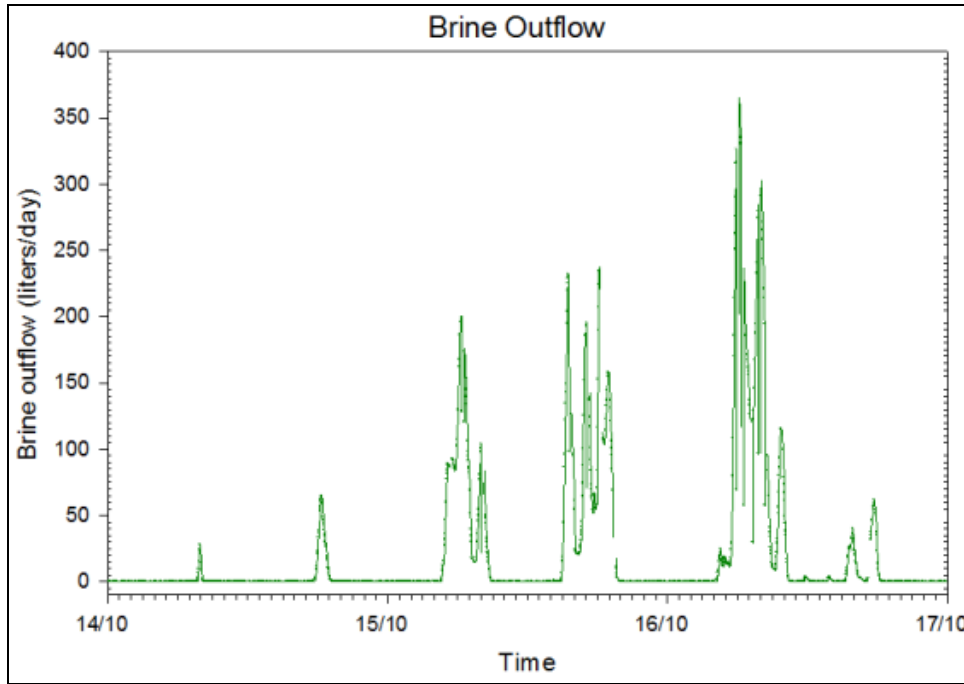
Figure 10. Fluctuations of the brine out-flow rate during a 3-day long period.

Because cavern brine pressure is halmostatic during the test, *permeation and leaks* are considered to be negligible. (The cavern pressure has remained halmostatic for 30 years; fast transient leak rates, sometimes observed at the beginning of a Mechanical Integrity Test, when a large pressure increase suddenly is applied in the cavern, were not expected during the SG13-SG14 test.)

The magnitude of *atmospheric pressure fluctuations* is several hPa per day. Cavern compressibility is approximately $\beta V = 130$ m^3/MPa or, more conveniently when atmospheric pressure fluctuations are considered, $\beta V = 13$ liters/hPa : one can expect that pressure fluctuations generate large changes in the brine-outflow rate, whose average value is 12 liters/day.

In fact, the ratio between the brine-outflow rate and atmospheric pressure fluctuations (or bV) is not exactly the same as the ratio between the injected brine flow and the cavern pressure increase, or $\beta V = 13$ litres/hPa. This is because, in sharp contrast to pressure changes during a compressibility test, atmospheric pressure applies an additional load both on the brine/air interface in the well, resulting in cavern expansion/contraction, *and* on the ground surface, resulting in a change in geostatic stresses and a contraction/expansion of the cavern.

It is also known that *ground-level temperature fluctuations*, with a period of 24 hours, and Earth tides, with periods of 12 hours-25 minutes and 24 hours, may have significant influence on cavern behavior (see, for example, Bérest et al., 2006). Typically, Earth tides generate cavern volume changes that are in the range 10^{-8}-10^{-7}, or 2.4 to 24 liters in a $V = 240,000$ m^3 cavern.

Brouard et al. (2009) performed an analysis of these phenomena in the case of the SG13-SG14 caverns; they proved that atmospheric pressure variations and, to a smaller extent, Earth tides, explain the observed brine outflow fluctuations.

3.9. Conclusions

A liquid-outflow test was performed in the SG13-14 cavern of the Gellenoncourt brine field. Brine outflow from the cavern was measured over a 190-day period. Brine outflow is a geyser-

like phenomenon: fast brine rates (several hundreds of liters/day) are followed by long periods of time during which no flow is expelled from the cavern. However, the average brine flow-rate is representative of the cavern-creep closure rate, which is 12 liters/day or

$$\dot{V}/V = 5.8 \times 10^{-13} \text{ s}^{-1} = 1.8 \times 10^{-5} \text{ yr}^{-1}$$

Even though slow (Total cavern closure is reached after 55,000 years.), this rate is significantly faster than expected. As noted in Section 1.2, for a sample submitted to an uniaxial stress $\sigma = 10$ MPa , a typical range of strain rates was

$$10^{-11} \text{ s}^{-1} < \dot{\varepsilon}^{ss}_{10 \text{ MPa}} < 10^{-9} \text{ s}^{-1}$$

Consider now an idealized spherical cavern at a 250-m depth (approximately the depth of the SG13-SG14 caverns). When formula (3) is accepted,

$$\left.\frac{\dot{V}}{V}\right|^{NH}_{ss} = -\frac{3}{2} A * \left[\frac{3}{2n}\left(P_\infty - P_c\right)\right]^n = -\frac{3}{2}\left(\frac{3}{2n}\right)^n \left(\frac{P_\infty - P_c}{10}\right) \dot{\varepsilon}_{10 \text{ MPa}}$$

The steady-state volumetric convergence rate of such a cavern should be

$$3 \times 10^{-14} \text{ s}^{-1} < \dot{V}/V < 3 \times 10^{-12} \text{ s}^{-1} \quad \text{when } n = 3$$

and

$$3.6 \times 10^{-17} \text{ s}^{-1} < \dot{V}/V < 3.6 \times 10^{-15} \text{ s}^{-1} \text{ when } n = 5$$

Gellenoncourt salt is not known as an especially creep-prone salt. [Creep properties of rock salt from the neighboring Varangéville Mine were studied by G. Vouille (unpublished). The cavern convergence rate predicted from Vouille's tests is 1 liter/day ($\dot{V}/V = 5 \times 10^{-14} \text{ s}^{-1}$), and 2 liters / day when the transient phase due to an initial small decompression of the cavern is taken into account — i.e., slower by one order of magnitude than the measured convergence rate.]

CONCLUSIONS

The findings at this stage can be summarized as follows.

1. Strong theoretical and experimental evidence supports the view that fluid-assisted deformation plays a significant role in laboratory creep tests, especially when applied deviatoric stresses are small (say, smaller than $\sigma = 5$ MPa).

2. Simple calculations prove that closure rate of actual salt caverns is influenced strongly by phenomena affecting rock salt in the $\sigma < 5$ MPa deviatoric stress domain.

3. Few creep tests have been performed on natural salt samples in the stress range of interest ($\sigma < 5$ MPa); these tests strongly suggest that the creep rate is much faster than the rate extrapolated from empirical laws fitted to test results performed in the $\sigma \approx 5$ to 10 MPa deviatoric stress domain.

4. In-situ data are scarcer still. A brine outflow test was performed in a 250-m deep cavern of the Gellenoncourt brine field in Eastern France. The cavern closure rate is faster than expected.

Additional data still are needed. However, from these results, it seems plausible that the creep closure rate of shallow salt caverns could be faster than generally is believed, with significant consequences, for example, when cavern abandonment is considered.

ACKNOWLEDGEMENTS

REFERENCES

Bérest P., Bergues J. and Brouard B. (1999) - *Static and dynamic compressibility of deep underground caverns*. Int. J. Rock Mech. & Mining Sci., 36:1031-1049.

Bérest P., Blum P.A., Charpentier J.P., Gharbi H. and Valès F. (2005) - *Very slow creep tests on rock samples.* Int. J. Rock Mech. & Mining Sci., 42, 569-576.

Bérest P., Brouard B., Karimi-Jafari M. and Van Sambeek L. (2007) - *Transient behaviour of salt caverns. Interpretation of Mechanical Integrity Tests*. Int. J. Rock Mech. Min. Sc. 44, pp. 767-786,.

Bérest P., Karimi-Jafari M., Brouard B. and Bazargan B. (2006) - *In Situ Mechanical Tests in Salt Caverns*. Proc. SMRI Spring Meeting, Brussels, 91-129.

Bérest P., Bergues J., Brouard B., Durup J.G. and Guerber B. (2001) *A salt cavern abandonment test*. Oil & Gas Journal, Rev. IFP, Vol. 56, 5:541-469.

Bérest B., Brouard B. and Karimi-Jafari M. (2008) *The effect of small deviatoric stresses on cavern creep behavior*. Proc. SMRI Fall Meeting, Austin, p. 296-310.

Blum W. and Fleischmann C. (1988) - *On the deformation-mechanism map of rock salt.* Proc. 2nd. Conf. Mech. Beh. of Salt. Clausthal-Zellerfeld, Germany: Transactions of Technical Publishers, 7-23.

Breunesse J.N., van Eijs R.M.H.E, deMeer S. and Kroon I.C. (2003) - *Observation and prediction of the relation between salt creep and land subsidence in solution-mining-The Barradeel case.* Proc. SMRI Fall Meeting Chester, 38-57.

Brouard B., Bérest P., Héas J.Y, Fourmaintraux D., de Laguérie P. and You T. (2004) - *An in situ test in advance of abandoning of a salt cavern*. Proc. SMRI Fall Meeting, Berlin, Germany 45-64.

Brouard B., Lheur C., Hertz E., Bérest P., de Greef V., Béraud J.F. (2009) - *A brine-outflow test in a Gellenoncourt cavern*. Proc. SMRI Spring Meeting, Krakow.

Buffet A. (1998) - *The collapse of Compagnie des Salins SG4 and SG5 drillings. Proc. SMRI Fall Meeting*, Roma, p. 79-105.

Campos de Orellana A.J. (1998) - *Non-Associated Pressure Solution Creep in Salt Rock Mines*. Proc. 4th Conf. Mech. Beh. of Salt, Transactions of Technical Publishers, 429-444.

Clerc-Renaud A. and Dubois D. (1980) - *Long-term Operation of Underground Storage in Salt.* Proc.5th Symp. on Salt, Coogan A.H. and Hauber L. ed., the Salt Institute, Vol. II, 3-10.

Gaulke K., Rokhar R., Staudmeister K., Zander-Schiebenhofer D. (2007) - *Reassessment of the Creep Behaviour of the Rustringen Salt dome for Optimization and Future Development of the Crude Oil Cavern Storage Facility*. Proc. SMRI Meeting, Halifax, Canada, p.155-172.

Hugout B. (1988) - *Mechanical behavior of salt cavities -in situ tests- model for calculating the cavity volume evolution*. Proc. 2nd Conf. Mech. Beh. of Salt, Hannover, September 1984. Trans Tech Pub., Clausthal-Zellerfeld, Germany, 291–310.

Hunsche U. (1984) - *Results and interpretation of creep experiments on rock salt*. Proc. 1st Conf. Mech. Beh. of Salt. Clausthal-Zellerfeld, Germany: Transactions of Technical Publishers, 159-167.

Hunsche U. (1988) - *Measurement of creep in rock salt at small strain rates. Proc. 2nd Conf. Mech. Beh. of Salt* Clausthal-Zellerfeld, Germany: Transactions of Technical Publishers, 187-196.

Langer M. (1984) - *The rheological behaviour of rock salt*. Proc. 1st Conf. Mech. Beh. of Salt. Clausthal-Zellerfeld, Germany: Transactions of Technical Publishers, 201-240.

Munson D.E. and Dawson P.R.(1984) - *Salt constitutive modeling using mechanism maps*. Proc. 1st Conf. Mech. Beh. of Salt. Clausthal-Zellerfeld, Germany: Transactions of Technical Publishers, 717-737.

Spiers C.J., Schutjens P.M.T.M., Brzesowsky R.H., Paech C.J., Liezenberg J.L. and Zwart H.J. (1990) - *Experimental determination of the constitutive parameters governing creep of rocksalt by pressure solution*. In: Knipe R.J. and Rutter E.H.(eds) Deformation Mechanisms, Rheology and Tectonics. Geological Society special Publication 54: 215-227.

Uraï J.L. and Spiers C.J. (2007) - *The effect of grain boundary water on deformation mechanisms and rheology of rocksalt during long-term deformation*. Proc. 6th Conf. Mech. Beh. of Salt, Taylor & Francis Group, 149-158.